Electrochemical and Solid-State Letters, **13** (6) H173-H175 (2010)
1099-0062/2010/13(6)/H173/3/$28.00 © The Electrochemical Society

Effects of Mg Additive on Inhibition of Ag Agglomeration in Ag-Based Ohmic Contacts on p-GaN

Yang Hee Song, Jun Ho Son, Gwan Ho Jung, and Jong-Lam Lee*,z

Division of Advanced Materials Science, Department of Materials Science and Engineering, Pohang University of Science and Technology, Pohang, Gyeongbuk 790-784, Korea

We investigate the effect of Mg additive on the inhibition of Ag agglomeration in Ag contacts on p-GaN. The Mg-containing Ag contact shows low contact resistivity of 6.3×10^{-5} Ω cm^2, high reflectance of 85.5% at 460 nm wavelength, and better thermal stability than the Ag contact after annealing in air ambient. Synchrotron radiation photoemission spectroscopy revealed that Mg atoms dissolving in the Ag contact reacted with oxygen atoms to form Mg oxides and increases the work function via decreasing the Schottky barrier height for hole injection. This leads to the inhibition of Ag atoms from lattice diffusion in the contact and to the suppression of the formation of Ag agglomeration, leading to enhanced light reflectance and thermal stability.
 [DOI: 10.1149/1.3355164]

Manuscript submitted November 9, 2009; revised manuscript received January 19, 2010. Published March 16, 2010.

In vertical-structure GaN-based light emitting diodes (LEDs),[1-3] the p-type ohmic contact with low contact resistivity and high reflectance is essential to enhance the light extraction and reduce the power consumption. Silver (Ag) has been widely used for reflective ohmic contacts due to the high reflectance (~95%) in visible wavelength and low contact resistivities on the order of 10^{-5} Ω cm^2 by annealing in oxygen ambient.[3,4] However, Ag contacts were agglomerated during annealing in air ambient, leading to degradation in electrical and optical properties.[5,6] Therefore, preventing Ag contacts from agglomeration is a key aspect in realizing high power LEDs of solid-state lighting.

Regarding the physical origin of Ag agglomeration, two different mechanisms have been suggested, including surface diffusion to reduce the total free energy and bulk diffusion of Ag atoms by oxygen–vacancy interaction.[7,8] The thermal stability of the Ag-based contacts could be enhanced using surface passivation and epitaxial growth of Ag film due to the reduction in the surface diffusion.[5,9,10] However, the Ag agglomeration still occurred because of the remaining oxygen–vacancy interaction in the contact. To reduce the oxygen–vacancy interaction, it is essential to reduce oxygen atoms dissolved in the lattice of the Ag contact.

In this article, we study the suppression of Ag agglomeration by Mg additive to form Mg oxides and therefore to reduce oxygen content in the Ag contact. Adding Mg additive to Ag contact, the specific contact resistivity, light reflectance, and surface morphology of the contact were significantly improved. Interfacial reactions between contact metals and GaN, and the formation of Mg oxide, were analyzed using synchrotron radiation photoemission spectroscopy (SRPES).

Mg-doped p-GaN grown on (0001) sapphire using metallorganic chemical vapor deposition was used. For measurements of specific contact resistivity using the transmission line method, active regions were defined by inductively coupled plasma, followed by dipping samples into a boiling aqua regia solution to remove surface oxides.[11] Then, 200 nm thick Mg-containing Ag contact [Ag(Mg)] was deposited on the p-GaN by electron-beam evaporation under a pressure of 3×10^{-7} Torr. A Ag–Mg alloy target containing 0.1 wt % Mg was made by electron-beam melting. The samples were annealed at temperatures ranging from 300 to 500°C for 1 min in air. The current–voltage characteristics of the contacts were examined using a semiconductor parameter analyzer. The reflectance of the contacts was measured using a tungsten–halogen lamp, a monochromator, and a Ag mirror with the certified reflectance of 95% in the interest wavelength as a reflectance standard.

Table I shows contact resistivities and light reflectance for Ag and Ag(Mg) contacts with annealing temperature. The Ag contact shows the lowest contact resistivity of 3.0×10^{-5} Ω cm^2 after annealing at 300°C and increases rapidly at a higher temperature. The Ag(Mg) contact shows the lowest contact resistivity of 2.2×10^{-5} Ω cm^2 at 400°C and gradually degrades at a higher temperature. The reflectance of the Ag contact degrades to 71.8% after annealing at 400°C. Meanwhile, the reflectance of the Ag(Mg) contact slowly degrades with annealing temperature and shows 82.6% at 400°C.

Figure 1 shows the changes in contact resistivities (ρ_c) and light reflectance as a function of annealing time at 300°C. The contact resistivity of each sample is normalized with minimum resistivity (ρ_o) before annealing and is plotted as ρ_t/ρ_o. For the Ag contact, the value of ρ_t/ρ_o drastically increases by a factor of 1300 after annealing for 60 min, but the Ag(Mg) contact has increased about 8 times. The light reflectance of the Ag contact decreases to 57% after annealing at 300°C for 30 min, but the reflectance of the Ag(Mg) contact is as high as 86%. These results demonstrate that the Mg additive in the Ag contact has a role in suppressing the degradation of Ag(Mg) contact, resulting in better thermal stability.

Figure 2a and b shows the SRPES spectra of Ga 3d core levels of Ag and Ag(Mg) contacts. For the as-deposited contacts, the Ga 3d peak is composed of Ga–N and Ga–O bonds. However, after annealing, the peak is deconvoluted into three bonds, corresponding to Ga–N, Ga–O, and metallic Ga bonds. The binding energy differences of 1.2 ± 0.1 eV between the Ga–O and Ga–N bonds and 0.9 ± 0.1 eV between the Ga–N and metallic Ga bonds agree well with the previously reported values.[12] The peak intensity of metallic Ga bonds significantly increases, and the Ga 3d peak of both contacts shifts to lower binding energy after annealing. In particular, the binding energy shift of the Ag(Mg) contact is significant. These results mean that the amount of metallic Ga in the Ag(Mg) contact is larger than that in the Ag contact.

Figure 3 shows SRPES spectra of Mg 2p core levels for Ag(Mg) contacts before and after annealing. For the as-deposited contact, the Mg 2p spectrum is mainly composed of the Mg–Ag bond. However, after annealing, the full width at half-maximum value of the peak increased from 1.28 to 1.61 eV. This means that an additional bonding is imposed in the Mg 2p spectra, deconvoluted into two bonds, corresponding to Mg–O and Mg–Ag bonds. The binding energy difference of 1.0 ± 0.1 eV between the Mg–O and Mg–Ag bonds agrees well with the previously reported values.[12] This provides that Mg oxide was produced in the Ag(Mg) film during the annealing. Also, Mg concentration is calculated from the Mg 2p and Ag 3d peaks. The quantitative concentration is obtained by dividing the integrated peak area by atomic sensitivity factors.[13] This method provides that the Ag(Mg) contact contains 0.1 wt % Mg atoms.

Figure 4a and b exhibits the spectra of the secondary electron photoemission for Ag and Ag(Mg) contacts before and after annealing. In both contacts, the onsets shift toward a higher work function after annealing. However, the shift is more pronounced in the

* Electrochemical Society Active Member.
z E-mail: jllee@postech.ac.kr

Table I. Changes in contact resistivity and reflectance for Ag and Ag(Mg) contacts as a function of annealing temperature.

	Ag		Mg-containing Ag	
Annealing temperature (°C)	Contact resistivity (Ω cm^2)	Reflectance (%)	Contact resistivity (Ω cm^2)	Reflectance (%)
As-deposited	1.8×10^{-2}	94	9.8×10^{-3}	93.8
300	3.0×10^{-5}	88.8	2.9×10^{-4}	89.6
350	1.7×10^{-4}	81.7	6.3×10^{-5}	85.5
400	6.8×10^{-4}	71.8	2.2×10^{-5}	82.6
450	7.8×10^{-3}	58.6	8.4×10^{-5}	80.4
500	2.4×10^{-2}	49.9	1.9×10^{-4}	78.1

Ag(Mg) contact (0.19 eV) than in the Ag contact (0.07 eV). This suggests that Mg atoms dissolved in Ag film reacted with oxygen to produce Mg oxides, resulting in the increase in the work function by $\Delta E = 0.12$ eV.

The surface morphologies of Ag and Ag(Mg) contacts after annealing by scanning electron microscopy (SEM) and atomic force microscopy (AFM) are shown in Fig. 5. The annealed Ag contact shows a very irregular surface morphology and several holes due to Ag agglomeration.[7] For the Ag(Mg) contact, the surface roughness is a little increased, but no holes are found after annealing. AFM phase images show that the grain sizes of the Ag(Mg) contact are smaller than those of the Ag contact. The AFM results show that the Ag(Mg) contact suppresses the Ag agglomeration.

The ohmic formation mechanism of the Ag(Mg) contact can be explained with the formation of Ag–Ga solid solution and the increase in work function.[5] The formation of Ag–Ga solid solution leaves the Ga vacancies below the contact. Because Ga vacancies could act as shallow acceptors for electrons in GaN, the net hole concentration in the near-interface region increased, reducing the Schottky barrier height for the transport holes across the interface.[5] Also, the increase in work function means the decrease in hole injection barrier at the metal/GaN interface. In the Ag(Mg) contact, the dissolution of Ga atoms in Ag is more pronounced and the increase in work function is higher than that in the Ag one, resulting in lower contact resistivity than the Ag contact.

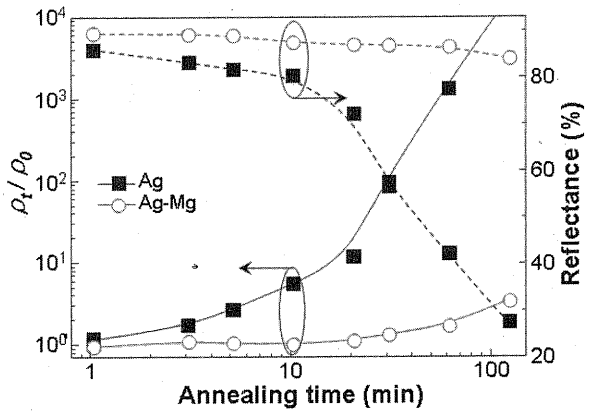

Figure 1. (Color online) Changes in (a) ρ_t/ρ_0 and (b) light reflectance at 460 nm wavelength for Ag and Ag(Mg) contacts as a function of annealing time at 300°C in air ambient.

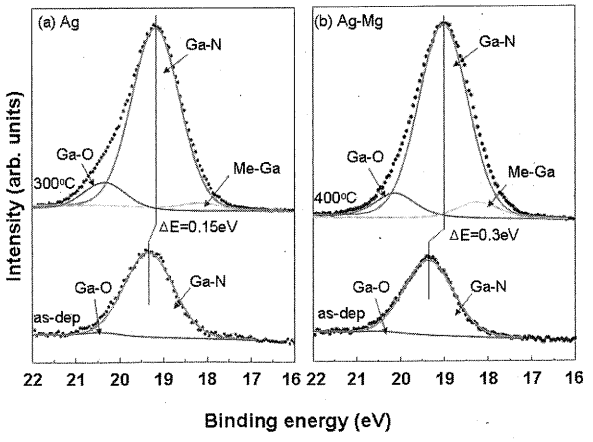

Figure 2. (Color online) SRPES spectra of Ga 3d core levels for (a) Ag (20 Å) contact before and after annealing at 300°C and (b) Ag(Mg) (20 Å) contact before and after annealing at 400°C for 1 min in air ambient.

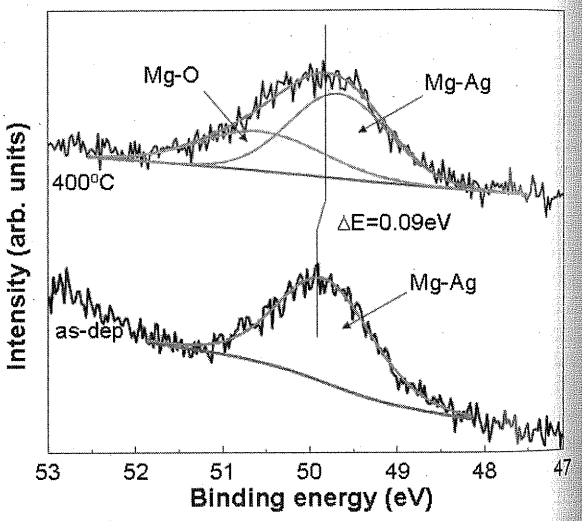

Figure 3. (Color online) SRPES spectra of Mg 2p core levels for Ag(Mg) (20 Å) contacts before and after annealing at 400°C for 1 min in air ambient.

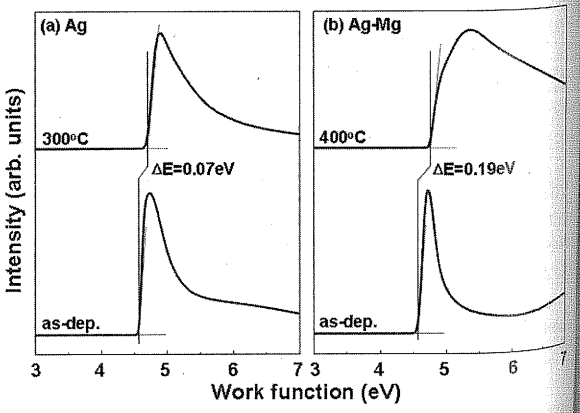

Figure 4. SRPES spectra of secondary electron emission for (a) Ag (20 Å) and (b) Ag(Mg) (20 Å) contacts before and after annealing.

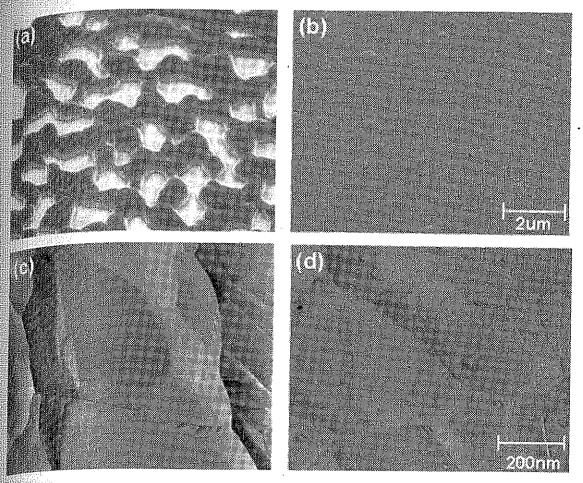

Figure 5. (Color online) SEM micrographs of (a) Ag contact and (b) Ag(Mg) contact after annealing at 400°C in air ambient. AFM phase images of (c) Ag contact and (d) Ag(Mg) contact after annealing at 400°C in air ambient.

The thermally stable Ag(Mg) ohmic contact is attributed to the suppression of Ag agglomeration by Mg atoms dissolved in Ag matrix. In the Ag–Mg phase diagram,[14] the solubility limit of Mg in Ag is 20 wt % at room temperature. Thus, Mg atoms (0.1 wt %) in the Ag matrix are randomly dispersed and then form the solid solution. This is compared with a recent result of Ag(Cu) contact, which produced CuO precipitation on grain boundaries due to the solubility difference between the eutectic point (780°C) and room temperature.[9] The Mg atoms have a large driving force for oxidation during annealing in air ambient because Gibb's free-energy changes for the formation of MgO and AgO at 400°C are −525.5 and 5.63 kJ/mol, respectively.[15] As a result, the formation of MgO is more favorable energetically than AgO, thus forming MgO during the annealing in air ambient. The self-diffusion of the Ag atom is enhanced as the concentration of vacancies in the Ag film increases, resulting in the Ag agglomeration.[16] The oxygen atoms, preferentially, were occupied at the substitution site of silver when Ag film was exposed to oxygen ambient.[8] Due to the strong interaction between oxygen atoms and vacancies, vacancies uptake the substitutional oxygen atoms into interstitial sites, leaving vacancies behind.[16] Therefore, the annealing in air ambient accelerates the Ag agglomeration more than in any other ambient such as nitrogen, helium, and Ar.[17] For the Ag(Mg) contact, owing to the large difference in oxygen affinity between Mg and Ag atoms, Mg atoms at substitutional sites preferentially make a chemical bond with oxygen atoms, occupying octahedral interstitial sites to form Mg oxides.[18] Thus, the formation of the oxygen–vacancy cluster is prohibited[16,18] because the number of oxygen atoms at substitutional sites is relatively reduced, resulting in the suppression of Ag agglomeration. As a result, good thermal stability in Ag(Mg) ohmic contact can be obtained, leading to a high reflectance and a smooth surface morphology.

In conclusion, Ag(Mg) ohmic contact showed a low contact resistivity of 2.2×10^{-5} Ω cm^2 and a high reflectance of 82.6% after annealing at 400°C in air. The excellent thermal stability in Ag(Mg) contact is attributed to the formation of Mg oxides in Ag film, which prohibits the formation of vacancies and prevents the Ag agglomeration. Therefore, it is suggested that Mg additive in Ag contact plays a critical role in enhancing the optical, electrical, and thermal stability of high power LEDs.

Acknowledgment

This work was supported by Priority Research Centers Program through the National Research Foundation of Korea (NRF) funded by the Ministry of Education, Science and Technology (2009-0094037) and in part by World Class University program through the National Research Foundation of Korea funded by the Ministry of Education, Science and Technology (project no. R31-2008-000-10059-0).

Pohang University of Science and Technology assisted in meeting the publication costs of this article.

References

1. W. K. Wang, S. Y. Huang, K. S. Wen, D. S. Wuu, and R. H. Horng, *Appl. Phys. Lett.*, **88**, 181113 (2006).
2. J. H. Son, H. K. Yu, Y. H. Song, and J.-L. Lee, *Electron. Mater. Lett.*, **4**, 157 (2008).
3. C. H. Chou, C. L. Lin, Y. C. Chung, H. Y. Bor, and C. Y. Liu, *Appl. Phys. Lett.*, **90**, 022103 (2007).
4. L.-B. Chang, C.-C. Shiue, and M.-J. Jeng, *Appl. Phys. Lett.*, **90**, 163515 (2007).
5. H. W. Jang, J. H. Son, and J.-L. Lee, *J. Electrochem. Soc.*, **155**, H563 (2008).
6. J.-O. Song, J. S. Kwak, Y. Park, and T.-Y. Seong, *Appl. Phys. Lett.*, **86**, 062104 (2005).
7. H. C. Kim, N. D. Theodore, and T. L. Alford, *J. Appl. Phys.*, **95**, 5180 (2004).
8. J.-P. Crocombette, H. Monestrol, and F. Willaime, *Phys. Rev. B*, **66**, 024114 (2002).
9. J. H. Son, G. H. Jung, and J.-L. Lee, *Appl. Phys. Lett.*, **93**, 012102 (2008).
10. J.-Y. Kim, S.-I. Na, G.-Y. Ha, M.-K. Kwon, I.-K. Park, J.-H. Lim, and S.-J. Park, *Appl. Phys. Lett.*, **88**, 043507 (2006).
11. J.-L. Lee, J. K. Kim, J. W. Lee, Y. J. Park, and T. Kim, *Solid-State Electron.*, **43**, 435 (1999).
12. J. F. Moulder, W. F. Strickle, P. E. Sobol, and K. D. Bomben, *Handbook of X-Ray Photoelectron Spectroscopy*, Perkin-Elmer, Eden Prairie, MN (1992).
13. G. A. Aricò, A. K. Shukla, H. Kim, S. Park, M. Min, and V. Antonucci, *Appl. Surf. Sci.*, **172**, 33 (2001).
14. T. B. Massalski, J. L. Murray, L. H. Bennett, and H. Baker, *Binary Alloy Phase Diagrams*, American Society for Metals, Metals Park, OH (1986).
15. I. Barin, F. Sauert, E. Schultze-Rhonhof, and W. S. Sheng, *Thermochemical Data of Pure Substances*, VCH, Weinheim (1989).
16. G. Mathieu, P. Gas, A. Combe-Brun, and J. Bernardini, *Acta Metall.*, **31**, 1661 (1983).
17. G. F. Malgas, D. Adams, P. Nguyen, Y. Wang, T. L. Alford, and J. W. Mayer, *J. Appl. Phys.*, **90**, 5591 (2001).
18. L. Charrin, P. Gergaud, G. Gonzalez, A. Mazuelas, and A. Charai, *Oxid. Met.*, **66**, 21 (2006).